Supporting Information

Table SI-1. Compositions of PGPs and PGFs expressed in atomic % measured via EDX.

Sample	P	Ca	Na	Mn	O
PGP-Mn0	20.5 ± 0.4	8.1 ± 0.2	4.1 ± 0.2	-	67.3 ± 0.9
PGP-Mn1	21.9 ± 0.4	6.2 ± 0.5	3.5 ± 0.3	0.2 ± 0.3	68.2 ± 0.4
PGP-Mn3	20.0 ± 0.3	7.4 ± 0.2	3.9 ± 0.4	0.6 ± 0.5	68.1 ± 1.1
PGP-Mn5	20.9 ± 0.4	6.9 ± 0.5	3.6 ± 0.5	1.0 ± 0.4	67.6 ± 0.5
PGP-Mn10	20.5 ± 0.5	6.6 ± 0.4	2.1 ± 0.2	2.2 ± 0.4	68.6 ± 1.0
PGF-Mn0	20.5 ± 0.8	6.5 ± 0.3	4.2 ± 0.5	-	68.8 ± 1.2
PGF-Mn1	20.7 ± 0.5	5.4 ± 0.4	4.2 ± 0.2	0.2 ± 0.4	69.5 ± 0.4
PGF-Mn3	20.8 ± 0.4	5.0 ± 0.5	3.2 ± 0.4	0.6 ± 0.4	70.4 ± 0.8
PGF-Mn5	21.8 ± 0.7	5.2 ± 0.2	1.7 ± 0.4	1.1 ± 0.5	70.3 ± 1.5
PGF-Mn10	22.3 ± 0.9	4.0 ± 0.4	1.2 ± 0.8	2.2 ± 0.3	70.3 ± 0.6

Table SI-2. Summary of key references on PGs.

Synthesis	*Morphology*	*TMI*	*Mol %*	*Cytocompatibility*	*Antimicrobial properties*	*Properties*	*Ref*
SG	Mesoporous PGP	Sr^{2+}	1-3-5			Pore size 11.8-18.6 nm. Specific Surface Area (SSA) 123-73 m^2/g. Sr^{2+} acts as a cross-linker. Good drug delivery system (DDS).	43
SG	Mesoporous PGP	Cu^{2+}	1-3-5		Antibacterial effect against *S. aureus* from day 1 (3 and 5 mol% of Cu2+). Activity against *E. coli* was for all compositions after day 2.	Pore size 8-20 nm. SSA 124-67 m^2/g. The role of Cu^{2+} changes from network modifying to network forming with increasing Cu^{2+} content. Good DDS.	*44*
SG	Mesoporous PGP	Zn^{2+}	1-3-5			Average pore size ~12 nm. SSA 124-76 m^2/g. Good DDS.	*45*
COA	PGP	Zn^{2+}	2-10-15	MTT assay on MG-63 and HaCaTs cells. Good cell viability of all PGs, with slightly reduced cell viability at higher loadings. ~ 100% for MG-63 ≥ 69% for HaCaTs		Zn^{2+} adopts a 6-coordinate geometry. Good DDS.	*42*
COA	PGP	Cu^{2+}	2-10-15	MTT assay on MG-63 and HaCaTs cells. Good cell viability of all PGs, with slightly reduced cell viability at higher loadings. ≥ 79% for MG-63 ≥73% for HaCaTs		Cu^{2+} adopts a 4-coordinate geometry. Good DDS.	*42*
ES-COA	PGF	Cu^{2+}	1-3-5	Cu^{2+} enhancement of MG-63 viability and proliferation.	Cu^{2+} has antibacterial activity against *S. aureus* and *E. coli*.	PGFs average diameter 1-3 µm. Cu^{2+} acts as cross-linker.	*13*
ES-COA	PGF	Ag^{+}	1-2-4-6-10	Dissolution products non-toxic against HaCaTs. Enhancment of wound closure in *ex vivo* models, (≥ 4 mol % Ag^{+}) HaCaT migration/proliferation demonstrated by *in vitro* scratch assays sstarting from PGF-Ag6, reaching 72% closure with 10 mol % Ag^{+}.	PGF-Ag (Ag_2O ≥ 4 mol%) antibacterial activity against *S. aureus* and *E. coli.*	PGFs average diameter 4.2 µm. Good DDS.	*9*
ES-COA	PGF	Zn^{2+}	1-2-4-6-10	Dissolution products non-toxic against HaCaTs.	PGF-Zn10 antibacterial activity against *S. aureus*	PGFs average diameter: 1.4 µm. Good DDS.	*9*
ES-COA	PGF	Fe^{3+}	1-2-4	Dissolution products are non-toxic against HaCaTs. Acceleration of healing in chronic wounded skin via *ex vivo* assay (> 30%) on1 mol% Fe.		PGFs average diameter 5.2 µm. Good DDS.	*9*
ES-COA-SUP	Porous PGF	Ga^{3+}	0.2-0.5-1	All PGF dissolution products are non-toxic against HaCaTs.	PGFs have antibacterial activity against *E. coli*. 1 mol% Ga^{3+} has antibacterial activity against *S. aureus.*	Pores diameters from 100 nm to 2 µm. Ga^{3+} acts as cross-linker. All PGFs are able to encapsulate clove oil (99.99 %). Clove oil is mostly released within the first 6 hours. The presence of Ga^{3+} promotes the release of clove oil. Clove oil and Ga^{3+} enhanced the antioxidant properties of PGFs.	*14*

COA = coacervation; ES-COA = ES of the coacervate gel; ES-COA-SUP = ES of the coacervate gel combined with the supramolecular templating technique

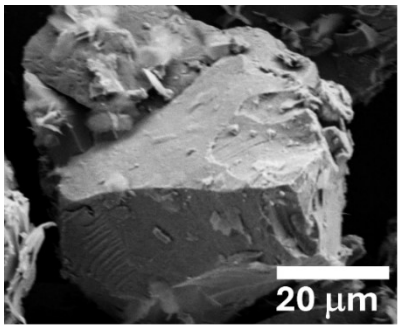

Figure SI-1. SEM image of PGP-Mn1

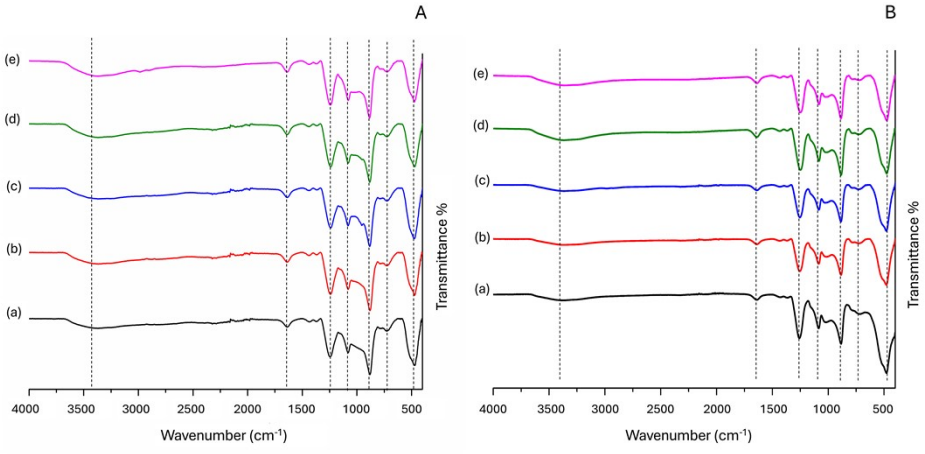

Figure SI-2. FT-IR spectra of A): (a) PGP-Mn0; (b) PGP-Mn1; (c) PGP-Mn3; (d) PGP-Mn5; (e) PGP-Mn10 and B): (a) PGF-Mn0; (b) PGF-Mn1; (c) PGF-Mn3; (d) PGF-Mn5; (e) PGF-Mn10.

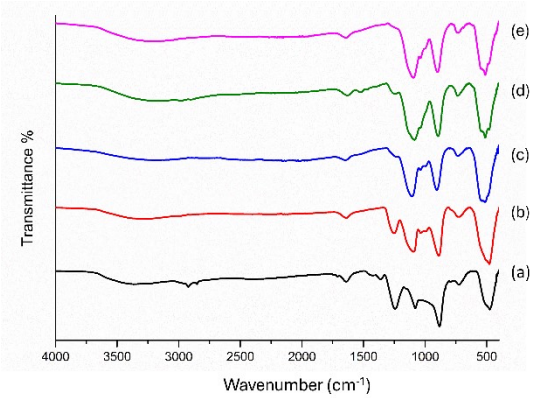

Figure SI-3. FT-IR spectra of PGP-Mn1 before (a) and after immersion in CM for 24 h (b), 72 h (c) and after immersion in Tris-B for 24 h (d), 72 h (e).